

Methods

A UPLC-MS/MS method for quantification of metabolites in the ethylene biosynthesis pathway and its biological validation in *Arabidopsis*

Da Cao¹ , Thomas Depaepe¹ , Raul Sanchez-Muñoz¹ , Hilde Janssens² , Filip Lemière³, Tim Willems⁴ , Johan Winne² , Els Prinsen⁴  and Dominique Van Der Straeten¹ 

¹Laboratory of Functional Plant Biology, Department of Biology, Faculty of Sciences, Ghent University, 9000, Ghent, Belgium; ²Department of Organic Chemistry, Polymer Chemistry Research Group and Laboratory for Organic Synthesis, Ghent University, 9000, Ghent, Belgium; ³Department of Chemistry, Biomolecular and Analytical Mass Spectrometry, University of Antwerp, 2020, Antwerp, Belgium; ⁴Integrated Molecular Plant Physiology Research, Department of Biology, University of Antwerp, 2020, Antwerp, Belgium

Summary

Authors for correspondence:
Dominique Van Der Straeten
Email: dominique.vanderstraeten@ugent.be

Els Prinsen
Email: els.prinsen@uantwerpen.be

Received: 11 April 2024
Accepted: 14 May 2024

New Phytologist (2024)
doi: 10.1111/nph.19878

Key words: 1-aminocyclopropane-1-carboxylic acid, ethylene biosynthesis, glutamyl-ACC, jasmonyl-ACC, malonyl-ACC, method validation, synthetic chemistry of standards, UPLC-MS/MS quantification method.

- The plant hormone ethylene is of vital importance in the regulation of plant development and stress responses. Recent studies revealed that 1-aminocyclopropane-1-carboxylic acid (ACC) plays a role beyond its function as an ethylene precursor. However, the absence of reliable methods to quantify ACC and its conjugates malonyl-ACC (MACC), glutamyl-ACC (GACC), and jasmonyl-ACC (JA-ACC) hinders related research.
- Combining synthetic and analytical chemistry, we present the first, validated methodology to rapidly extract and quantify ACC and its conjugates using ultra-high-performance liquid chromatography coupled to tandem mass spectrometry (UPLC-MS/MS). Its relevance was confirmed by application to *Arabidopsis* mutants with altered ACC metabolism and wild-type plants under stress.
- Pharmacological and genetic suppression of ACC synthesis resulted in decreased ACC and MACC content, whereas induction led to elevated levels. Salt, wounding, and submergence stress enhanced ACC and MACC production. GACC and JA-ACC were undetectable *in vivo*; however, GACC was identified *in vitro*, underscoring the broad applicability of the method.
- This method provides an efficient tool to study individual functions of ACC and its conjugates, paving the road toward exploration of novel avenues in ACC and ethylene metabolism, and revisiting ethylene literature in view of the recent discovery of an ethylene-independent role of ACC.

Introduction

Ethylene, a gaseous phytohormone, holds a pivotal role in the regulation of plant growth and development (Depaepe & Van Der Straeten, 2020; Pattyn *et al.*, 2021). 1-aminocyclopropane-1-carboxylic acid (ACC) serves as the direct biosynthesis precursor of ethylene. ACC is derived from *S*-adenosyl-L-methionine by ACC synthases (ACS), which is a crucial and a main rate-limiting step in ethylene biosynthesis (Boller *et al.*, 1979; Yang & Hoffman, 1984). Subsequently, ACC is transformed into ethylene through the catalytic action of ACC oxidases (ACO; Hamilton *et al.*, 1990; Barry *et al.*, 1996).

In addition to its direct role in ethylene production, ACC can form conjugates with various metabolites in plants. It has been proposed that ACC conjugates contribute to the regulation of the active pool of ACC, maintaining ACC homeostasis in

response to diverse environmental conditions (Vanderstraeten & Van Der Straeten, 2017; Pattyn *et al.*, 2021). Three distinct types of ACC conjugates have been identified so far, which are malonyl-ACC (MACC; Amrhein *et al.*, 1981; Hoffman *et al.*, 1982; Hoffman *et al.*, 1983), glutamyl-ACC (GACC; Martin *et al.*, 1995; Peiser & Yang, 1998) and jasmonyl-ACC (JA-ACC; Staswick & Tiryaki, 2004). Among them, MACC is thought to be the major ACC metabolite *in planta*, with its endogenous level being *c.* 5–260-fold higher than ACC depending on the plant species and developmental stages (Hoffman *et al.*, 1983; Sarquis *et al.*, 1992; Peiser & Yang, 1998; Bulens *et al.*, 2011; Van de Poel *et al.*, 2012). As such, MACC is proposed to be a storage form of ACC (Bouzayen *et al.*, 1988). GACC and JA-ACC, instead, are likely to have more specific functions. GACC may be involved in the regulation of early osmotic stresses, while JA-ACC was supposed to be more engaged in biotic stress responses

(Li *et al.*, 2019; Pattyn *et al.*, 2021), but could be linked to abiotic stress responses as well, since both ethylene and jasmonates are related to abiotic stresses (Kazan, 2015). However, none of these hypotheses have been conclusively proven, partly due to the challenges associated with measuring these compounds (Vanderstraeten & Van Der Straeten, 2017). In addition, recent studies have uncovered a role for ACC as a signaling molecule independent from its conversion to ethylene (Vanderstraeten *et al.*, 2019; Mou *et al.*, 2020; D. Li *et al.*, 2022), making the need for accurate determination of ACC and its conjugates, in conjunction with ethylene levels, more imminent.

Despite the identification of ACC and its conjugates in plant tissues more than four decades ago, the absence of chemical standards and low endogenous levels has hindered the development of a validated method for their simultaneous extraction and quantification. The original method for ACC quantification, termed the Lizada–Yang procedure, was indirect and made use of the chemical oxidation of ACC to ethylene, and subsequent quantification by gas chromatography (GC) with flame ionization detection (Boller *et al.*, 1979; Lizada & Yang, 1979). The first direct ACC measurement was achieved by paper chromatography (Grady & Bassham, 1982), followed by liquid chromatography coupled with UV detector (LC-UV; Lanneluc-Sanson *et al.*, 1986) and GC coupled mass spectrometry (GC-MS; Savidge *et al.*, 1983, Smets *et al.*, 2003). GC-MS has also been applied for the identification of MACC, GACC, and JA-ACC in wheat, tomato, and *Arabidopsis* individually (Hoffman *et al.*, 1982; Martin *et al.*, 1995; Staswick & Tiryaki, 2004). However, due to the absence of pure standards and internal standards, absolute quantification of ACC conjugates has never been achieved. Nowadays, ultra-high-performance liquid chromatography coupled with tandem mass spectrometry (UHPLC-MS/MS) has become the most sensitive and efficient approach for phytohormone identification and quantification (Pan *et al.*, 2010; Šimura *et al.*, 2018; Cao & He, 2023; Dixon & Dickinson, 2024) and has also been applied for the quantification of ACC (Chauvaux *et al.*, 1997; Müller & Munné-Bosch, 2011; Ziegler *et al.*, 2014). However, all of these methods lack the capability to quantify ACC conjugates. In addition, some require a time-consuming solid-phase extraction (SPE) and/or derivatization procedure before UHPLC-MS/MS analysis in order to enhance MS sensitivity or facilitate UHPLC separation. To date, there is no validated direct method allowing for the simultaneous extraction and quantification of ACC and its conjugates from plant tissues. Such methodology could greatly facilitate comparative analyses of ACC and its conjugates to enable thorough insight into ACC metabolism.

Combining synthetic and analytical chemistry, the current study successfully yielded pure standards of ACC conjugates and presents a novel method enabling rapid and simultaneous extraction and quantification of four types of ACC-related metabolites without derivatization or SPE. The method was applied to quantify the concentrations of ACC and ACC-related metabolites in *Arabidopsis* wild-type (WT) and various ACC-biosynthesis mutants under abiotic stress or treated with an ACC-biosynthesis inhibitor. The results show unambiguous evidence supporting

the feasibility and accuracy of this method and provide valuable insights for the investigation of the ACC and ethylene metabolic pathways in plants. Given the recent discovery of a signaling role of ACC, apart from ethylene, this method serves as an invaluable tool to get to grips with the distinct functions of ACC and its conjugates and comprehensively reevaluate the ethylene field in view of the ethylene-independent function of ACC. In addition, this technique will be a precious aid in the detailed identification and characterization of the genes encoding the elusive conjugates forming the three known ACC derivatives. Therefore, this methodology bears the potential to have great impact in the ethylene field.

Materials and Methods

Chemicals

ACC and aminoethoxyvinyl glycine (AVG) were purchased from Merck (Hoeilaart, Belgium). JA-ACC was custom synthesized by ABClabatory Scientific Co. Ltd, Hangzhou, China (CAS No. 371778-55-1). MACC and GACC are synthesized as detailed in Supporting Information Notes S1, and their purities were validated by NMR as shown in Notes S2. Isotope-labeled internal standards (ISTDs) including 2-amino- $[\text{2H}_3]$ 4-methylsulfanylbutanoic acid (d_3 -methionine) and $[\text{2H}_4]$ 1-aminocyclopropanecarboxylic acid (d_4 -ACC) were sourced from Merck and Olchemim (Olomouc, Czech Republic), respectively. The molecular weight and purity of all synthesized standards were confirmed by the collision-induced dissociation (CID) spectra obtained by UPLC-MS/MS using a 0.1 mM aqueous reference solution, except for GACC for which a 1 mM solution was used, due to the relatively lower MS sensitivity for GACC (Fig. 1). All solvents used were LC-MS grade purchased from Merck (Belgium).

Plant material and growth conditions

Arabidopsis thaliana L. Heynh. Col-0 (WT), *acs7x*, and *acs8x* (Tsuchisaka *et al.*, 2009) were purchased from the Nottingham Arabidopsis Stock Center (NASC). *eto1-1* (Wang *et al.*, 2004) and *eto3-1* (Chae *et al.*, 2003) were acquired from the Arabidopsis Biological Resource Center (ABRC). *aco2-1*, *aco2aco4*, *etf-1*, and *etf-2* seeds were provided by courtesy of Jan Hejatko (Central European Institute of Technology) and Li-Jia Qu (Peking University; W. Li *et al.*, 2022, Yamoune *et al.*, 2023). *jar1-1* was sourced from the European Arabidopsis Stock Center NASC (Staswick *et al.*, 2002). Surface-sterilized seeds were plated on half-strength Murashige and Skoog medium ($\frac{1}{2}$ MS) supplemented with 1% sucrose and 0.8% agar (Murashige & Skoog, 1962). Then, seeds were vernalized for 3 d at 4°C in dark conditions. After vernalization, seeds were transferred to a growth chamber to germinate and grow vertically under long-day conditions (16 h : 8 h, light : dark, $21 \pm 2^\circ\text{C}$ day : night temperature, 60% humidity, light intensity $70\text{--}90 \mu\text{mol m}^{-2} \text{s}^{-1}$) for 2 wk except where specified otherwise. Col-0 plants were also germinated and grown for 14 d on plates supplemented with AVG. AVG was dissolved in sterile water and added to the medium at

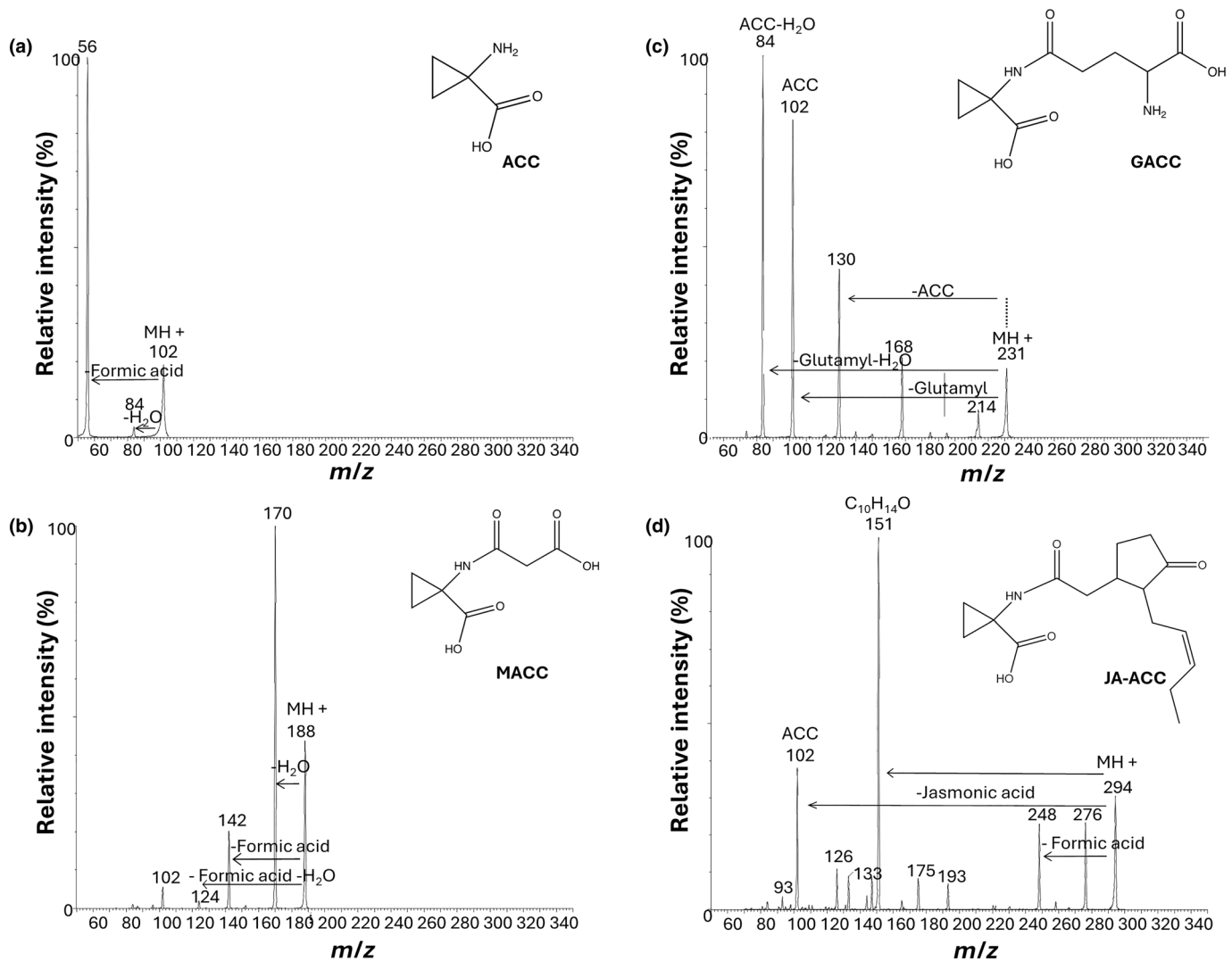


Fig. 1 Collision-induced dissociation spectra and predicted fragment structures of 1-aminocyclopropane-1-carboxylic acid (ACC) and its conjugates using UPLC-ES(+)-MS/MS. (a) ACC, (b) malonyl-ACC (MACC), (c) glutamyl-ACC (GACC), and (d) jasmonyl-ACC (JA-ACC). Spectra were obtained using a 10^{-4} M reference solution, except for GACC for which we used 10^{-3} M.

different final concentrations (0.1–10 μ M). Plants were imaged after 14 d using a Canon EOS 550D camera (Canon, Tokyo, Japan). For sample harvest, plant leaves and roots were collected separately, snap-frozen in liquid nitrogen, and stored at -80°C until sample extraction.

For stress treatments, 14-d-old plantlets were used. For osmotic and salt stresses, plantlets were transferred to $\frac{1}{2}$ MS containing 150 mM mannitol or 100 mM NaCl, respectively. Flooded plants were totally submerged, and for wounding stress, all leaves were clipped using tweezers. After transfer to the stress condition, plants were kept in the same light and temperature conditions as described above. For cold and heat treatments, plantlets were incubated at 4°C or 37°C , respectively, under the same light regime. All stress conditions were maintained for 24 h, except for heat stress, which was limited to 3 h. After treatment, plant leaves and roots were harvested separately as described above.

In vitro assay for GACC formation

Crude protein was extracted from 0.5 g of *Nicotiana benthamiana* leaves as reported previously (Martin *et al.*, 1995). Briefly, 1.5-ml extraction buffer (100 mM Tris-HCl pH 8.0, 10% glycerol, 50 mM EDTA, and 40 mM 2-mercaptoethanol) was added to 0.5-g homogenized leaf tissue and sonicated at 50% amplitude (6 cycles of 10 s ON and 30 s OFF). Then, samples were centrifuged at 15 900 rcf at 4°C for 15 min and the supernatant was stored at -80°C until *in vitro* assay performance. To produce GACC, 100 μ l of crude protein extract was incubated with 400 μ l of potassium phosphate buffer at the indicated pH values, varying between pH 5 and 8 (supplemented with 5 mM 2-mercaptoethanol and 5 mM EDTA) with or without 200 μ M ACC. Samples were incubated at 30°C for 24 h, and the reaction was stopped by adding 100 μ l 1 M HCl.

Table 1 Selected multiple reaction monitoring parameters for ACC and related conjugates and corresponding internal standards under positive mode with two different columns.

Full name	Abbreviation	Standard type	Column type	Q1	Q3	CE
1-aminocyclopropane-1-carboxylic acid	ACC	Standard	BEH amide	102	56	15
				102	84	10
Glutamyl-ACC	GACC	Standard	HSS T3	231.5	84	10
				231.5	130, 168	10
Malonyl-ACC	MACC	Standard	HSS T3	188.2	170	15
				188.2	142, 124	25
Jasmonyl-ACC	JA-ACC	Standard	HSS T3	294.3	151	21
				294.3	248, 276	15
d ₄ -ACC	d ₄ -ACC	Internal standard	BEH amide	106	60	15
				106	88	10
d ₃ -methionine	d ₃ -methionine	Internal standard	HSS T3	153.1	136	17
				153.1	107	20

The transitions selected for quantification are highlighted in bold. Q1, precursor ion selected in Q1 (the first quadrupole mass filter); Q3, product ion selected in Q3 (the second quadrupole mass filter); ACC, 1-aminocyclopropane-1-carboxylic acid; BEH amide, bridged ethylene hybrid (BEH) amide column; CE, collision energy; GACC, glutamyl-ACC and JA-ACC, jasmonyl-ACC; HSS T3, High Strength Silica T3 column; MACC, malonyl-ACC.

Sample extraction

Around 100 mg of homogenized frozen plant material was accurately weighed and extracted with 1 ml 50% (v/v) methanol containing 0.05 μM d₄-ACC and 1 μM d₃-methionine as internal standards. The sample was vortexed for 10 s and stored at 4°C for 1 h. Subsequently, the sample was centrifuged at 15 900 rcf at 4°C for 5 min, and the supernatant was filtered with an Amicon[®] 3 kDa MWCO centrifugal filter (cellulose pore size 3 kDa nominal molecular weight limit; Millipore, Darmstadt, Germany) before UPLC-MS/MS analysis. The extract can be concentrated further to enhance sensitivity. For *in vitro* assays, the reaction solution was injected to UPLC-MS/MS directly after spiking with ISTDs and purification with an Amicon 3 kDa filter.

Metabolite quantification with UPLC-MS/MS

The UPLC-MS/MS system was a Waters ACQUITY UPLC[®] (Waters, Milford, MA, USA) combined with an Sciex API 4000 MS (Foster City, CA, USA). ACC was separated on Waters ACQUITY UPLC[®] BEH (bridged ethylene hybrid) amide column (2.1 \times 150 mm, 130 Å, 1.7 μm), which enables hydrophilic interaction chromatography (HILIC). The ACC conjugates, including MACC, GACC, and JA-ACC, were separated on a Waters ACQUITY UPLC[®] HSS T3 Column (2.1 \times 150 mm, 100 Å, 1.8 μm). UPLC columns were maintained at 45°C, and the autosampler was maintained at 4°C. Mobile phase A was 0.1% FA in Milli-Q water; mobile phase B was 0.1% formic acid in acetonitrile. The flow rate was 0.4 ml min⁻¹. For ACC separation on the BEH amide column, the 9 min mobile phase gradient was 91% B over 0.5 min, 91–51% B over 5.5 min, followed by a clean-up step: 51–20% B over 1.5 min, 20% to 91% B over 0.5 min and column re-equilibration for 1 min. For ACC conjugate separation on the HSS TS column, the 9.5 min mobile phase gradient was 0% B over 1 min, 0–100% B over 6.5 min, followed by a clean-up step: isocratic

elution at 100% B for 1 min, 100% to 0% B over 0.1 min and column re-equilibration for 0.9 min. ESI parameters were as follows: scan mode: positive; collision gas: 8; curtain gas: 35 psi; ion source temperature: 500°C; ion source gas 1 and 2: 50 psi; Ion Spray voltage: 5500 V; resolution of Q1 and Q3: unit. The scheduled transitions monitored in multiple reaction monitoring (sMRM), and the corresponding parameters for all analytes and corresponding ISTDs are listed in Table 1.

Method validation

A pooled biological quality control (PBQC) sample consisting of a mixture of WT Arabidopsis shoots from six individual plants was generated for method validation, extracted as mentioned above for sample extraction. A standard mixture was spiked into PBQCs before and after extraction to achieve a final spiked concentration of 0.05 μM for ACC and JA-ACC, 0.1 μM for GACC, and 0.4 μM for MACC according to their endogenous contents in plant material (Peiser & Yang, 1998). The accuracy was calculated by comparing the calculated concentration of spiked analytes in PBQCs to the nominal value in six replicates (Verstraete *et al.*, 2021; Kumar *et al.*, 2022). The recovery was calculated by comparing the calculated concentration of spiked analytes in PBQCs before and after extraction in six replicates (Verstraete *et al.*, 2021). ISTD-corrected matrix effect was evaluated by comparing peak areas of samples spiked postextraction to spiked pure solvents in five replicates. The selectivity was calculated by comparing analyte ion ratios between spiked PBQCs and pure standard solutions in five replicates (WADA, 2010). The linearity range of each compound was determined by injecting 6 μl of compound mixes containing equimolar concentrations of all ACC metabolites, ranging from 0.1 nM to 1 mM, including d₄-ACC and d₃-methionine. Within the concentration range tested, we selected an optimal linear range excluding the lowest and highest concentrations for which data exceeded 20% deviation ($n = 5$). For the calibration curves, we spiked a calibration curve with a fixed concentration of both internal standards,

based on the amount used to spike samples. The ratio between the peak intensities of the unlabeled ($AREA_x$) and labeled ($AREA_{dx}$) compound of interest is plotted in function of the ratio between the concomitant concentrations in the reference mix injected.

Data analysis

Raw UPLC-MS/MS data were analyzed using ANALYST v.1.6.2 (AB Sciex, Foster City, CA, USA). Analyte levels were quantified based on the peak area ratios of endogenous compounds to corresponding ISTDs and the standard/ISTD ratios calculated using pure standards. GRAPHPAD PRISM v.10 (GraphPad Software, Boston, MA, USA) was used for statistical analysis, and the applied statistical tests were specified for each dataset within the Results section. For multiple comparisons, Fisher's least significant difference (LSD) test after one-way ANOVA was applied for datasets that passed the homoscedasticity (Brown–Forsythe test) and normality test (Shapiro–Wilk and D'Agostino–Pearson omnibus tests). Unpaired *t*-test with Welch's correction after Brown–Forsythe and Welch ANOVA was applied for datasets that passed the normality test but did not comply with the homoscedasticity requirement. Dunn's multiple comparisons test was used after the Kruskal–Wallis test whenever the dataset did not fulfill either the homoscedasticity or the normality requirement. The raw data supporting this study have been provided in Dataset S1.

Results

MS/MS method development and optimization

Collision-induced dissociation spectra of the protonated molecular ions were obtained for ACC and its conjugates and are presented in Fig. 1. The different fragments were annotated based on full exact mass scans and product ion scans (Table S1). The protonated molecular ions were selected as parent ions in Q1 (the first quadrupole mass filter), whereas for each compound, the two most abundant stable product ions were selected in Q3 (the second quadrupole mass filter) as diagnostic transitions under MRM. For each compound, the most abundant transition was selected for quantification, whereas the second transition was selected for confirmation. The transitions selected and collision settings after tuning are summarized in Table 1.

UPLC method optimization

For UPLC method optimization, both reversed-phase and normal-phase HPLC columns were tested, given the divergence in polarity of the different analytes. Specifically, a modified C18-based column for polar compound retention (Waters ACQUITY UPLC[®] High Strength Silica (HSS) T3 column) was tested for reversed-phase chromatography, and a Waters ACQUITY UPLC[®] BEH amide column was tested for normal-phase chromatography. HSS T3 displayed effective separation for all analytes, except for ACC, which eluted early due to its high polarity (Fig. 2b). Early elution of this very small molecule led to

incorrect quantification within complex plant matrices, particularly due to quenching and interfering polar compounds (Tables 2, S2). Therefore, the BEH amide column showing good retention of ACC was chosen for ACC quantification and HSS T3 was chosen for the quantification of ACC conjugates (Fig. 2b, c). [²H₄]1-aminocyclopropane-1-carboxylic acid (*d*₄-ACC) was used as the internal standard for ACC quantification, whereas due to the lack of ISTDs for ACC conjugates, *d*₃-methionine was used for the quantification of ACC conjugates.

Method validation

In order to evaluate the isotope dilution method for quantification, using *d*₄-ACC and *d*₃-methionine as internal standards, we investigated to what extent the concentration of the endogenous compound of interest can differ from that of the internal standard spiked to the extract. This enables a calculation based on the use of an internal tracer, omitting the need of an external standard curve. For this purpose, we composed a calibration curve with a fixed concentration of both internal standards. The ratio between the peak intensities of the unlabeled ($AREA_x$) and labeled ($AREA_{dx}$) compound of interest was plotted in function of the ratio between the concomitant concentrations in the reference mix (Fig. S1). These curves show a significant linear fit within the range shown. We advise to estimate the amount of internal standard within the same range as the expected amount in tissue and to respect a maximum deviation of 1/100 or 100/1. Both the *d*₄-ACC and *d*₃-methionine standards provided a good estimation of recovery and ionization efficiency for all ACC conjugates, for which no labeled standard is available. According to the retention time (Fig. 2b), and the calibration curves (Fig. S1), we can conclude that *d*₃-methionine is a good proxy as internal standard for ACC conjugates taking into account the respective correction factors as a measure for the compound-specific differences in ionization efficiency and specific responses of the diagnostic transition selected for quantification.

The linearity of MRM using the diagnostic transitions given in Table 1 is plotted in Fig. S2. For jasmonyl-ACC, linearity ranges between 10⁻⁸ M and 10⁻⁵ M corresponding to, respectively, 0.6 pmol and 0.6 μmol injected on column. The sensitivity for GACC and MACC is lower, both ranging from 10⁻⁶ to 10⁻³ M. For ACC, linearity ranged between 10⁻⁷ M and 10⁻⁴ M. All data were corrected for minor fluctuations in injection and ionization using the internal standard added to the equimolar mixes of the pure reference compounds.

The accuracy, recovery, selectivity, matrix effect, limit of detection (LOD), and limit of quantification (LOQ) were tested for method validation in an Arabidopsis matrix (US-FDA, 2018). To address the absence of a blank matrix, a spiking experiment using a PBQC Arabidopsis shoot sample was conducted to investigate the accuracy, recovery, selectivity, and matrix effect as reported previously (Cao *et al.*, 2020; Verstraete *et al.*, 2021). The accuracy (%bias) for all analytes was below 15% and the recovery ranged from 104% to 135% when the BEH amide column was used for the quantification of ACC, and the HSS T3 column for ACC conjugates (Table 2). HSS T3 showed poor

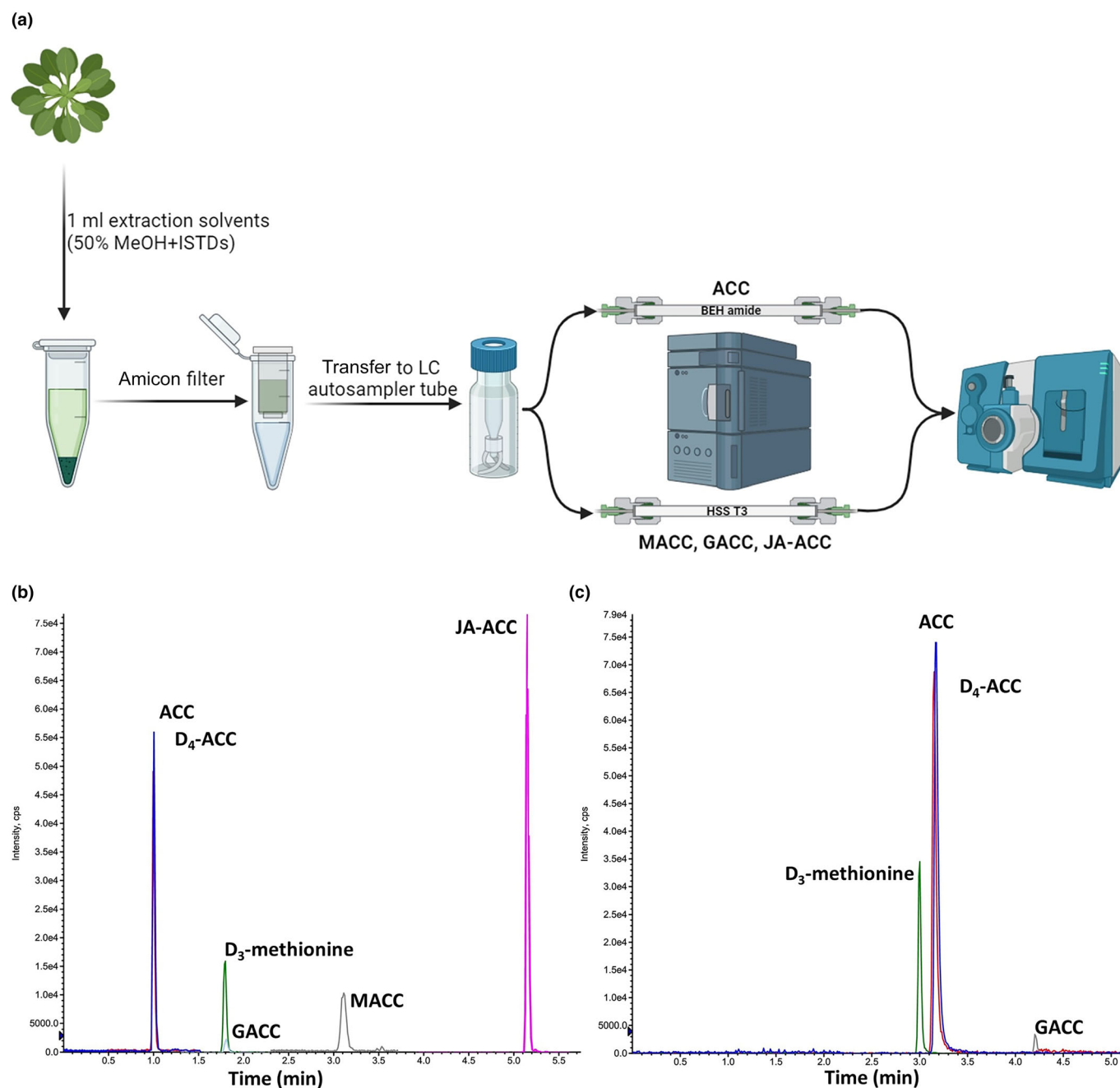


Fig. 2 Method workflow (a) and UPLC-MS/MS chromatogram showing the separation of ACC metabolites using High Strength Silica (HSS) T3 column (b) and bridged ethylene hybrid (BEH) amide column (c). A standard mixture containing 1 μM each of the analytes dissolved in 50% methanol was used. ACC, 1-aminocyclopropane-1-carboxylic acid; GACC, glutamyl-ACC; ISTDs, isotope-labeled internal standards; JA-ACC, jasmonyl-ACC; MACC, malonyl-ACC.

accuracy and recovery for ACC quantification, indicating the incorrect quantitation of ACC attributed to the matrix effect in plant matrices and inefficient separation of ACC on a C18-based column (Table 2; Fig. 2a). The ISTD-corrected matrix effects were 86% for MACC and JA-ACC, and 114% for ACC and GACC (Table 2). LOD and LOQ were set at a signal-to-noise ratio (S/N) of 3 and 10, respectively. The S/N was calculated using the Analyst software (Sciex, Foster City, CA, USA). Due to

the inability to detect GACC and JA-ACC in Arabidopsis extracts, spiked PBQC was used for the calculation of S/N. The LOQ for all analytes ranged from 0.02 to 177 nmol g^{-1} fresh weight (FW) and LOD values were in the range of 0.006–53 nmol g^{-1} FW. Regarding selectivity, no interferences were observed when a BEH amide column was used for the quantification of ACC neither for ACC conjugate quantification on an HSS T3 column. The ion ratios of all analytes in nonspiked and

Table 2 Accuracy, recovery, matrix effect, limit of detection (LOD), and limit of quantification (LOQ) for the developed UPLC-MS/MS methods.

Metabolite	Column	Accuracy (% bias)	Recovery		Matrix effect		LOD nmol g ⁻¹ FW	LOQ nmol g ⁻¹ FW
			%	RSD%	(%)	RSD%		
ACC	BEH amide	11	104	6	114	17	0.006	0.02
ACC	HSS T3	-69	30	166				
MACC	HSS T3	-11	124	21	86	17	0.4	1.2
JA-ACC	HSS T3	-14	135	6	86	6	0.001	0.004
GACC	HSS T3	13	110	23	114	23	53	177

The accuracy was calculated by comparing the calculated concentration of spiked analytes in pooled biological quality controls (PBQCs) to the nominal value. The recovery was calculated by comparing the calculated concentration of spiked analytes in PBQCs before and after extraction, $n = 5$. The LOD and LOQ were calculated as signal-to-noise ratio at 3 and 10, respectively. ACC, 1-aminocyclopropane-1-carboxylic acid; FW, fresh weight; GACC, glutamyl-ACC; JA-ACC, jasmonyl-ACC; MACC, malonyl-ACC; RSD, relative SD.

spiked PBQC samples were within the tolerance window calculated from pure standard solutions (Table S2). The use of an HSS T3 column for ACC quantification resulted in poor selectivity due to strong signal interferences, failing to meet the predefined criteria as outlined by WADA (2010) (Table S2), further supporting the choice of a BEH amide column for optimal and accurate quantification of ACC.

Method application

After method development, we applied our protocol to quantify ACC and its conjugates across various biological settings, including mutants in ACC and ethylene biosynthesis, as well as different stress conditions, anticipating changes in levels according to established knowledge. ACC and its conjugates were determined in the shoot and root tissue of WT (Col-0) Arabidopsis plants, treated with or without the ACS inhibitor AVG (Figs 3, S3). In addition, a variety of ethylene biosynthesis Arabidopsis mutants with either reduced ACC synthesis (*acs1-1acs2-1acs4-1acs5-2acs6-1acs7-1acs9-1* (*acs7x*, multiple loss-of-function mutant) and *acs2-1acs4-1acs5-2acs6-1acs7-1acs9-1amiRacs8acs11* (*acs8x*, multiple loss-of-function mutant)), increased ACC synthesis (*eto1-1* and *eto3-1*, gain-of-function mutants), or reduced ethylene synthesis (*aco2-1*, *aco2aco4*, *ethylene-free-1* (*etf-1*), and *etf-2*, *aco quintuple loss-of-function mutants*) were assayed (Chae *et al.*, 2003; Wang *et al.*, 2004; Tsuchisaka *et al.*, 2009; W. Li *et al.*, 2022; Yamoune *et al.*, 2023). We identified and quantified ACC and MACC in shoot and root tissues, with MACC showing remarkably higher concentrations in both tissues as compared to those obtained for ACC (ninefold higher in shoots and 59-fold in roots of Col-0 plants; Fig. 3a–d). The suppression of ACC synthesis achieved either via a pharmacological approach with AVG, a widely used inhibitor of ACS, or using higher-order knockout mutants of ACSs, led to decreased concentrations of both ACC and MACC. Moreover, a clear dose-dependent downregulation of ACC and MACC levels was noted with increasing AVG concentrations (ranging from 0.1 to 10 μ M). The ACC concentrations even dropped below the LOD in roots after 10 μ M AVG treatment as well as in roots of the ACS knockout mutants *acs7x* and *acs8x* (Fig. 3b). Conversely, roots of mutants with enhanced stability of certain ACSs, including *eto1-1* and *eto3-1*, showed significantly

higher concentrations of ACC and MACC as compared to Col-0 roots. While similar increases were observed in shoots, these differences were not statistically significant for ACC. Finally, *ACO* loss-of-function mutants were expected to accumulate more ACC, due to reduced conversion to ethylene. While the levels in single and in double loss-of-function *aco* mutants did not significantly differ from that in Col-0 plants, indicating functional redundancy, the quintuple knockouts *etf-1* and *etf-2* showed significantly higher concentrations of ACC and MACC in both shoots and roots. With respect to tissue specificity, shoots accumulated higher levels of ACC compared with roots, while, at least in Col-0 plants, the opposite trend was observed for MACC.

Given the well-known involvement of ethylene in abiotic stress responses (Kazan, 2015), we also quantified the levels of ACC and its conjugates in Arabidopsis shoots exposed to a range of abiotic stresses, including osmotic stress, salt stress, complete submergence, and wounding stress for 24 h (Fig. 3e,f). In these conditions, ACC concentrations exhibited a slight yet nonsignificant increase under osmotic and wounding stresses, while salt and submergence treatments led to significant increases in ACC (Fig. 3e). MACC levels, instead, exhibited an overall increase across all treatments with the submergence treatment showing the most notable rise compared with the control (Fig. 3f). However, since all treatments lasted 24 h and since it is known that ethylene levels peak within a shorter time period (*c.* 12 h) after wounding treatment returning to the control level after 24 h (Li *et al.*, 2018; Nieuwenhuizen *et al.*, 2021), we further performed a short-term wounding treatment. A rapid increase in ACC was observed after 1 h of treatment (Fig. 3g). This significant increase was enhanced throughout the 3 h time course. MACC did not show any changes, except for an increase after 2 h of treatment (Fig. 3h). Apart from ACC and MACC, we also analyzed GACC and JA-ACC levels in all experimental setups. However, these metabolites were not detectable in the experiments described above.

As GACC and JA-ACC could not be detected in Arabidopsis plants *in vivo*, we performed an *in vitro* assay following the conditions under which GACC was originally discovered and characterized (Martin *et al.*, 1995; Peiser & Yang, 1998). A protein extract from *Nicotiana benthamiana* leaves was incubated with or

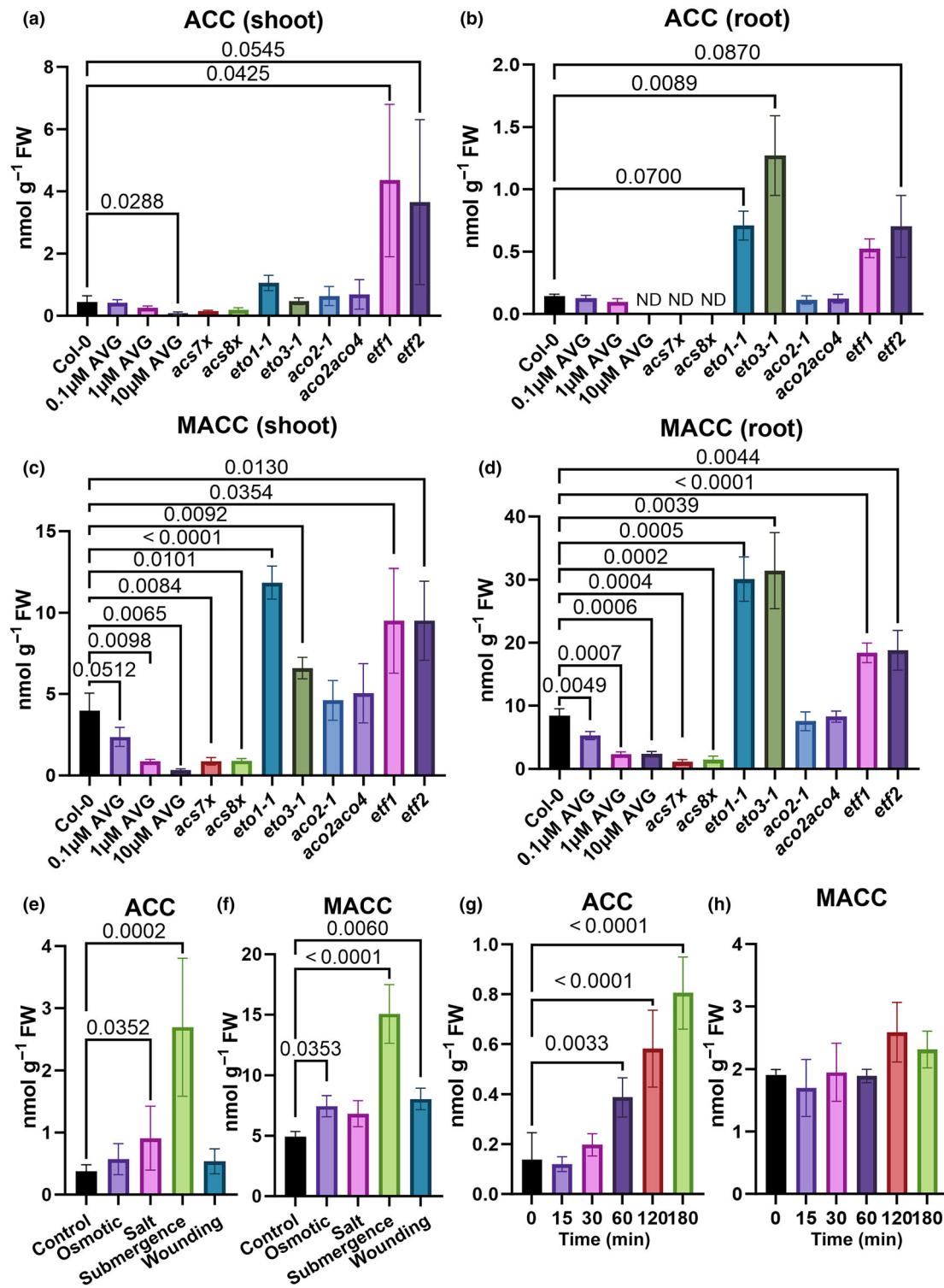


Fig. 3 ACC and MACC concentrations in diverse Arabidopsis samples, altered in ACC or ethylene biosynthesis and under stress conditions. (a–d) ACC and MACC concentrations in wild-type (WT) Arabidopsis plants (Col-0) treated with or without 0.1, 1, and 10 μM of the ACC-biosynthesis inhibitor aminoethoxyvinyl glycine (AVG), and in a range of ethylene biosynthesis mutants (*acs7x*, *acs8x*, *eto1-1*, *eto3-1*, *aco2-1*, *aco2aco4*, *etf1*, and *etf2*). The data are presented separately for shoots (a, c) and roots (b, d), $n = 2-4$. (e, f) ACC and MACC concentrations in WT Arabidopsis (Col-0) shoots under control, osmotic, salt, complete submergence, and wounding conditions for 24 h, $n = 5$. (g, h) ACC and MACC concentrations in WT Arabidopsis (Col-0) shoots at 0, 15, 30, 60, 120, and 180 minutes after wounding treatment. $n = 4$. Values are mean \pm SD. Comparisons were performed with Dunn's multiple comparisons test after the Kruskal–Wallis test for a, b, e, and f, or an unpaired *t*-test with Welch's correction after Brown–Forsythe and Welch ANOVA for c and d or Fisher's least significant difference test after one-way ANOVA for g and h. Adjusted *P*-values < 0.1 are indicated for each pair-wise comparison to controls. ACC, 1-aminocyclopropane-1-carboxylic acid; FW, fresh weight; MACC, malonyl-ACC; ND, not detectable.

without ACC at various pH levels. Without ACC feeding, both GACC and JA-ACC levels were below the LOD in the crude protein extract. However, upon supplementation with ACC, measurable amounts of GACC were formed, indicating the presence of ACC gamma-glutamyl transferase (GGT) activity. Intriguingly, the activity of GGT displayed a pronounced pH dependence, with optimal activity at pH 8 within the tested pH range of 5–8 (Fig. 4a). The addition of reduced glutathione (GSH) led to a further enhancement in GACC production, as illustrated in Fig. 4(b), with a modest 28% increase. This could be attributed to the presence of a sufficiently high endogenous GSH concentration, as previously observed in crude extracts of tomato fruit (Martin *et al.*, 1995).

To further investigate the presence of JA-ACC, we conducted an *in vitro* assay incubating a protein extract with 200 μ M JA and ACC. However, no JA-ACC was detectable under these conditions. To induce the formation of JA-ACC, we subsequently sprayed exogenous JA and ACC on WT and *jasmonate resistant 1* (*jar1-1*) Arabidopsis leaves. Yet again no JA-ACC was observed, indicating the absence of detectable JA-ACC levels in both the *in vitro* and *in vivo* conditions tested.

Discussion

Accurate quantification of ACC and its conjugates along with ethylene is essential to understand the regulatory mechanisms underlying ACC metabolism in the context of ethylene biosynthesis and beyond. The recent discovery of ACC functioning as a signal independent from ethylene both in vegetative and in generative growth (Xu *et al.*, 2008; Tsuchisaka *et al.*, 2009; Vanderstraeten *et al.*, 2019; Mou *et al.*, 2020), urges further research to reveal its biological roles in plants, and intertwining of ACC with ethylene metabolism at all developmental stages. This is of paramount importance given the role of ethylene not only in plant development but also in response to multiple biotic and abiotic stresses (Broekaert *et al.*, 2006; Abeles *et al.*, 2012; Sanchez-

Munoz *et al.*, 2024). In the latter, ethylene was demonstrated to play a pivotal role being relevant in the regulation of more than 50% of the genes in the abiotic stress gene core (Sanchez-Munoz *et al.*, 2024). In plant–bacteria interactions, deamination of ACC also has been shown to play a crucial role, further underscoring the importance of ACC metabolism *in planta* (Glick *et al.*, 1998; McDonnell *et al.*, 2009). With the analytical method proposed here, it will not only be possible to dive into the intricacies of interconversions of ACC forms in abiotic stress response, but also into the exchange of ACC and its conjugates as part of inter-kingdom interactions in ecosystems, both in the above- and belowground plant compartments.

Similar to other phytohormones, measuring ACC-related metabolites in plants is challenging partially because of their low concentrations, their chemical diversity, and because of the matrix effects in plant extracts (Cao & He, 2023). Currently, there is no existing method allowing rapid and accurate quantification of ACC and its conjugates. To overcome this challenge, a high-throughput method was developed to quantify ACC, MACC, GACC, and JA-ACC from 100 mg of Arabidopsis tissue. This method employs a straightforward extraction process without the need for SPE, derivatization, or further concentration. Additionally, two validated UPLC-MS/MS methods are presented to enable separate quantification of ACC and its conjugates (Fig. 2). This high-throughput method has demonstrated good accuracy (below 15% bias) and recovery (104–135%; Table 2) with a potential for incorporating the analysis of more phytohormones into the methodology (Cao *et al.*, 2017; Šimura *et al.*, 2018; Karady *et al.*, 2024). Even though it is challenging to synthesize stable ISTDs for all ACC conjugates, the absolute quantification of the compounds could be further enhanced by including isotope-labeled ACC conjugates as internal standards for ACC conjugates in future analyses.

The present method demonstrates the effective detection and quantification of ACC and MACC in Arabidopsis. The absolute concentration of ACC determined by our method aligns closely

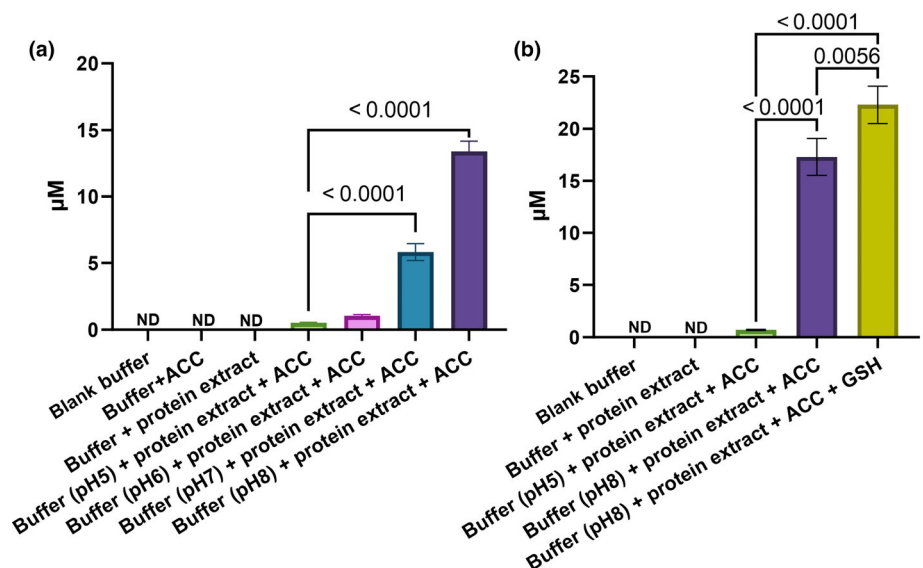


Fig. 4 Detection of glutamyl-ACC and assessment of ACC-glutamyl transferase activity in a crude *Nicotiana benthamiana* protein extract. The *in vitro* assay was performed by incubating crude protein extract from *Nicotiana benthamiana* leaves in a phosphate buffer at varying pH levels (5–8), supplemented with or without 200 μ M ACC (a) and 200 μ M reduced glutathione (GSH) (b). Blank buffer was at pH 8. Values are mean \pm SD, $n = 5$. Multiple comparison tests were performed with Fisher's least significant difference test after one-way ANOVA. Adjusted P -values < 0.1 were labeled for each comparison. ACC, 1-aminocyclopropane-1-carboxylic acid.

with previously reported ACC levels in WT *Arabidopsis* shoots which were *c.* 0.5 nmol g⁻¹ FW, affirming the accuracy of our methodology (Fig. 3a; Ziegler *et al.*, 2014, Karady *et al.*, 2024). Furthermore, our data indicated that suppressing *ACS* gene expression resulted in decreased ACC and MACC levels, while stabilizing *ACS* proteins or suppressing *ACO* expression increased the levels of ACC and MACC (Fig. 2a–d). These results correlate well with reported ethylene production in these mutants, hence providing further validation of the precision of our measurements (Chae *et al.*, 2003; Wang *et al.*, 2004; Tsuchisaka *et al.*, 2009; W. Li *et al.*, 2022). Notably, the level of ACC or MACC in quintuple *aco* mutants (*etf1* and *etf2*) exhibited a significant increase compared with WT plants, but *aco* single or double mutant (*aco2-1*, *aco2aco4*) did not show any significant changes. This observation suggests functional redundancy among *ACO* genes in *Arabidopsis*, similar to what has been reported for the *ACS* gene family (Tsuchisaka *et al.*, 2009; Houben & Van De Poel, 2019). Previous studies have noted that the ethylene overproducing mutants *eto1* and *eto3* manifest phenotypic differences compared with WT exclusively in roots under light-grown conditions (Rao *et al.*, 2002; Chen *et al.*, 2013; An & Gao, 2021). Correspondingly, our findings revealed that ACC accumulation in *eto1* and *eto3* as compared to WT was significant in roots, but not in shoots (Fig. 3a,b). Exposure to submergence and salt stress significantly enhanced the level of ACC, as previously reported, and of MACC (Fig. 3e,f; Van Der Straeten *et al.*, 2001, Tao *et al.*, 2015, Tamang *et al.*, 2021). These consistent results again reinforce the accuracy of our methodology. Interestingly, short-term wounding treatment revealed a rapid increase in ACC already significant at 60 min while exponentially increasing in the first 3 h by sixfold, returning back to the control level within 24 h (Fig. 3e,g). This corroborates the transient nature of ethylene emanation upon wounding, which peaks within 12 h before returning to baseline values (Li *et al.*, 2018; Nieuwenhuizen *et al.*, 2021). Furthermore, based on the results showing MACC accumulation upon wounding (Fig. 3f,h), we propose that the conversion of ACC to MACC is part of the regulatory mechanism of ethylene emanation in these conditions. At the early time points, while ACC rises steeply, no significant stable changes were observed for MACC. However, 24 h after wounding, MACC levels were significantly enhanced, demonstrating a form of metabolic feedback control over the conversion of ACC to ethylene (Fig. 3f,h).

It has been reported that *Arabidopsis* roots exhibit greater sensitivity to ACC and ethylene treatments as compared to shoots (Vanderstraeten *et al.*, 2019). Hence, it is anticipated that plants maintain relatively low endogenous ACC levels in roots. This is consistent with our findings (Fig. 3a,b). This could be explained by the fact that roots growing in a substrate, encounter partially hypoxic conditions depending on the depth and water content of the substrate (Hanslin *et al.*, 2005), leading to the accumulation of ACC (Bailey-Serres & Voesenek, 2008), while in parts of the root system which are in contact with a normal atmosphere, containing 21% oxygen, ethylene can accumulate more readily, potentially inhibiting ACC production through feedback regulation.

MACC is the first-identified conjugate of ACC and the major ACC conjugate in tomato (Amrhein *et al.*, 1981; Hoffman

et al., 1982, 1983; Peiser & Yang, 1998). The reported endogenous levels of ACC conjugates in different plant species vary *c.* 5–260-fold above their ACC levels, with MACC presumed to be the major contributor to this difference (Hoffman *et al.*, 1983; Sarquis *et al.*, 1992; Peiser & Fa Yang, 1998; Van de Poel *et al.*, 2012). Based on this assumption, MACC quantification has mostly been carried out indirectly after acid hydrolysis to ACC (Hoffman *et al.*, 1982, 1983; Sarquis *et al.*, 1992; Bulens *et al.*, 2011; Van de Poel *et al.*, 2012). With direct measurement of MACC, our study provides the first firm proof that MACC is the major ACC metabolite in *Arabidopsis* (Fig. 3). MACC showed remarkably higher amounts in both shoots and roots compared with ACC (ninefold higher in shoots and 59-fold in roots of WT plants; Fig. 3a–d). We herewith not only confirm the results obtained by paper chromatography after feeding radiolabeled ACC to tomato (Peiser & Yang, 1998), but also show that the actual content of both metabolites can be properly quantified.

MACC may act as a storage form of ACC and enables plants to fine-tune the ACC levels in different tissues (Vanderstraeten & Van Der Straeten, 2017). We observed that the MACC accumulation patterns in ACC-related mutants and in WT plants subjected to stresses are closely associated with changes in ACC levels (Fig. 3). Furthermore, MACC predominantly accumulated in *Arabidopsis* roots as compared to shoots (Fig. 3c,d), in contrast to ACC, which showed the opposite trend (Fig. 3a,b). These findings again underscore the importance of the balance between ACC and MACC. Roots are very sensitive to ACC, and MACC formation may act as a control point to keep intracellular ACC levels below a certain threshold. Moreover, the fact that MACC accumulation is closely associated with alterations in ACC levels supports the contention that MACC could act as a storage form. This is substantiated by the fact that MACC is stored in vacuoles, imported over the tonoplast membrane against its gradient (Bouzayen *et al.*, 1988). Functioning as a storage form implies the existence of enzymes carrying out MACC hydrolysis. Hoffman *et al.* (1983) reported that exogenous MACC has limited conversion into ACC in germinating peanut seeds. However, it is conceivable that the hydrolysis of MACC is insignificant during this particular developmental stage. It remains possible that MACC is merely a catabolite, acting as a product of the irreversible inactivation of ACC (Pattyn *et al.*, 2021). Exploring the potential conversion from MACC to ACC in future studies is intriguing, as much as the hunt for gene(s) encoding ACC malonyltransferase, forming MACC. The latter might function divergently across different cell types, contributing to the delicate equilibrium between MACC and ACC.

The other two known ACC conjugates, GACC and JA-ACC, remain more enigmatic. At present, it is unclear whether GACC exists in plants *in vivo* and, if it does, whether it accumulates at ultra-trace amounts or is rapidly metabolized. Previously, GACC was only detected in *in vitro* assays by incubating plant enzyme extracts with relatively high amounts of exogenous ACC (Martin *et al.*, 1995; Peiser & Yang, 1998). In the present study, we were able to detect GACC in a GACC-forming assay *in vitro* (Fig. 4; Martin *et al.*, 1995), but not in *Arabidopsis* nor in *Nicotiana*

benthiana leaves *in vivo*, not even upon feeding with ACC. Previous studies have examined additional plant species including tomato, vetch, mung bean, pea, wheat, peanut, and cotton, but in none of these GACC was detectable after ACC treatment (Hoffman *et al.*, 1982, 1983; Morris & Larcombe, 1995; Peiser & Yang, 1998). This raises the question whether GGT is capable of performing transferase activity to form GACC *in vivo*. GGT exhibits broad substrate specificity and can function both as a hydrolase and as a transferase *in vitro*, though exhibiting pH dependency (Lancaster & Shaw, 1994; Martin & Slovin, 2000). At pH 6, it predominantly acts as a hydrolase, while the transferase activity, forming GACC, increases with rising pH levels, reaching its peak at pH 8 or 9 (Fig. 4; Lancaster & Shaw, 1994; Martin & Slovin, 2000). Even though the average pH level in plant cells typically ranges from 6 to 7, this does not preclude the possibility of GACC synthesis by GGT occurring in specific subcellular locations with relatively high pH levels, such as mitochondria, or thylakoids, or under specific stresses, wherein pH variation is observed (Semenova, 2002; Shen *et al.*, 2013; Moreau *et al.*, 2021; Gámez-Arjona *et al.*, 2022). Therefore, it remains plausible that GACC exists *in vivo* and may accumulate in specific organelles or subcellular compartments, or is rapidly converted into another metabolite following its synthesis.

JA-ACC was initially detected in *Arabidopsis* with a concentration *c.* 18 pmol g⁻¹ FW (Staswick & Tiryaki, 2004). However, subsequent studies using sensitive methods failed to detect it, even with a reported LOD as low as 0.1 pmol g⁻¹ FW (Suza & Staswick, 2008; Koo *et al.*, 2009). In the present study, JA-ACC was undetectable in both *in vivo* and *in vitro* assays even after feeding with exogenous 200 µM jasmonic acid and ACC. Moreover, we attempted to perform the extraction process, combining two steps of SPEs and further concentration, as documented in the original paper by Staswick & Tiryaki (2004). Despite these efforts, we were unable to detect JA-ACC. Therefore, the existence of JA-ACC in plants remains unclear to date.

In conclusion, the first validated, efficient, and high-throughput method to quantify four types of ACC metabolites including ACC, MACC, GACC, and JA-ACC, was established. The method demonstrates good accuracy and recovery and has been successfully employed to measure ACC and its conjugates in various *Arabidopsis* mutants and WT plants subjected to abiotic stresses, as well as in *in vitro* conditions, biologically supporting the proposed analytical methodology. Moreover, this study reveals important novel physiological observations, particularly in relation to the metabolic equilibrium of ACC and its major conjugate MACC. The method will prove to be an invaluable tool to gain further insights into ACC and ethylene metabolism, which appear mutually dependent while also playing distinct roles in plant life. From this perspective, this methodology will have a significant impact on resolving key interactions in the plant biosphere, including numerous interactions with bacteria and fungi known to involve ethylene in the rhizo- and phyllosphere, as well as multiple abiotic interactions occurring in stressful environments (Nascimento *et al.*, 2018; Shekhawat *et al.*, 2022). In the current era of global climate change, the diverse forms of stress encountered by plants indeed are intricately linked with ethylene

(Sanchez-Munoz *et al.*, 2024). The methodology presented here offers the tools to assess the share of ACC therein, and genetically as well as molecularly characterize ACC metabolism. The time has come to revisit the ethylene field!

Acknowledgements

DVDS and EP gratefully acknowledge the Flanders Interuniversity Special Research Fund (iBOF, iBOF/23/070). DVDS is also grateful to the Research Foundation Flanders (FWO; G082421N) for funding, and to the Francqui Foundation for awarding her a Collen-Francqui Research Professorship (STI.DIV.2022.0014.01). RS-M is indebted to FWO (grant no.: 1288923N) for a senior postdoctoral fellowship. The authors also acknowledge the scientific and technical assistance of the Laboratory of Toxicology, Department of Bioanalysis, Faculty of Pharmaceutical Sciences, Ghent University, and Sevgi Öden of Antwerp University.

Competing interests

None declared.

Author contributions

DC, EP, FL and TW established the UHPLC-MS/MS method and calibration curves (Figs 1, 2, S1, S2; Tables 1, S1). DC validated the analytical method (Tables 2, S2). TD and RS-M performed the physiological experiments, after which DC measured the compounds and generated the datasets (Figs 3, 4, S3). HJ and JW performed synthesis and purification of the standards (Notes S1, S2), which DC, EP and FL characterized with MS (Fig. 1; Table S1). All authors were involved in data interpretation. DC, EP, TD, RS-M and DVDS wrote the manuscript, and all authors critically reviewed the manuscript. DVDS and EP designed experiments. Research coordination was performed by EP on the analytical part; DVDS took care of research coordination of the physiological part as well as of the overall coordination of the project.

ORCID

Da Cao  <https://orcid.org/0000-0001-7939-1048>

Thomas Depaepe  <https://orcid.org/0000-0003-2656-3437>


Hilde Janssens  <https://orcid.org/0000-0001-6764-7181>

Els Prinsen  <https://orcid.org/0000-0003-4320-1585>

Raul Sanchez-Muñoz  <https://orcid.org/0000-0003-0235-2985>

Dominique Van Der Straeten  <https://orcid.org/0000-0002-7755-1420>

Tim Willems  <https://orcid.org/0000-0002-2245-2126>

Johan Winne  <https://orcid.org/0000-0002-9015-4497>

Data availability

The raw data supporting this study are provided in Dataset S1.

References

- Abeles FB, Morgan PW, Saltveit ME Jr. 2012. *Ethylene in plant biology*. San Diego: Academic Press.
- Amrhein N, Schneebeck D, Skorupka H, Tophof S, Stöckigt J. 1981. Identification of a major metabolite of the ethylene precursor 1-aminocyclopropane-1-carboxylic acid in higher plants. *Naturwissenschaften* 68: 619–620.
- An C, Gao Y. 2021. Essential roles of the linker sequence between tetratricopeptide repeat motifs of ethylene overproduction 1 in ethylene biosynthesis. *Frontiers in Plant Science* 12: 657300.
- Bailey-Serres J, Voesenek L. 2008. Flooding stress: acclimations and genetic diversity. *Annual Review of Plant Biology* 59: 313–339.
- Barry CS, Blume B, Bouzayen M, Cooper W, Hamilton AJ, Grierson D. 1996. Differential expression of the 1-aminocyclopropane-1-carboxylate oxidase gene family of tomato. *The Plant Journal* 9: 525–535.
- Boller T, Herner RC, Kende H. 1979. Assay for and enzymatic formation of an ethylene precursor, 1-aminocyclopropane-1-carboxylic acid. *Planta* 145: 293–303.
- Bouzayen M, Latché A, Alibert G, Pech J-C. 1988. Intracellular sites of synthesis and storage of 1-(malonylamino) cyclopropane-1-carboxylic acid in *Acer pseudoplatanus* cells. *Plant Physiology* 88: 613–617.
- Broekaert WF, Delauré SL, De Bolle MF, Cammue BP. 2006. The role of ethylene in host-pathogen interactions. *Annual Review of Phytopathology* 44: 393–416.
- Bulens I, Van De Poel B, Hertog ML, De Proft MP, Geeraerd AH, Nicolai BM. 2011. Protocol: An updated integrated methodology for analysis of metabolites and enzyme activities of ethylene biosynthesis. *Plant Methods* 7: 17.
- Cao D, Barbier F, Yoneyama K, Beveridge CA. 2020. A rapid method for quantifying RNA and phytohormones from a small amount of plant tissue. *Frontiers in Plant Science* 11: 605069.
- Cao D, He M. 2023. Methods in phytohormone detection and quantification: 2022. *Frontiers in Plant Science* 14: 1235688.
- Cao D, Lutz A, Hill CB, Callahan DL, Roessner U. 2017. A quantitative profiling method of phytohormones and other metabolites applied to barley roots subjected to salinity stress. *Frontiers in Plant Science* 7: 2070.
- Chae HS, Faure F, Kieber JJ. 2003. The *eto1*, *eto2*, and *eto3* mutations and cytokinin treatment increase ethylene biosynthesis in *Arabidopsis* by increasing the stability of ACS protein. *Plant Cell* 15: 545–559.
- Chauvaux N, van Dongen W, Esmans EL, Van Onckelen HA. 1997. Quantitative analysis of 1-aminocyclopropane-1-carboxylic acid by liquid chromatography coupled to electrospray tandem mass spectrometry. *Journal of Chromatography A* 775: 143–150.
- Chen I-J, Lo W-S, Chuang J-Y, Cheuh C-M, Fan Y-S, Lin L-C, Wu S-J, Wang L-C. 2013. A chemical genetics approach reveals a role of brassinolide and cellulose synthase in hypocotyl elongation of etiolated *Arabidopsis* seedlings. *Plant Science* 209: 46–57.
- Depaepe T, Van Der Straeten D. 2020. Tools of the ethylene trade: a chemical kit to influence ethylene responses in plants and its use in agriculture. *Small Methods* 4: 1900267.
- Dixon RA, Dickinson AJ. 2024. A century of studying plant secondary metabolism—from “what?” to “where, how, and why?”. *Plant Physiology* 195: 48–66.
- Gámez-Arjona FM, Sánchez-Rodríguez C, Montesinos JC. 2022. The root apoplastic pH as an integrator of plant signaling. *Frontiers in Plant Science* 13: 931979.
- Glick BR, Penrose DM, Li J. 1998. A model for the lowering of plant ethylene concentrations by plant growth-promoting bacteria. *Journal of Theoretical Biology* 190: 63–68.
- Grady KL, Bassham JA. 1982. 1-aminocyclopropane-1-carboxylic acid concentrations in shoot-forming and non-shoot-forming tobacco callus cultures. *Plant Physiology* 70: 919–921.
- Hamilton A, Lycett G, Grierson D. 1990. Antisense gene that inhibits synthesis of the hormone ethylene in transgenic plants. *Nature* 346: 284–287.
- Hanslin HM, Sæbø A, Bergersen O. 2005. Estimation of oxygen concentration in the soil gas phase beneath compost mulch by means of a simple method. *Urban Forestry & Urban Greening* 4: 37–40.
- Hoffman NE, Fu J-R, Yang SF. 1983. Identification and metabolism of 1-(malonylamino) cyclopropane-1-carboxylic acid in germinating peanut seeds. *Plant Physiology* 71: 197–199.
- Hoffman NE, Yang SF, Mckee T. 1982. Identification of 1-(malonylamino) cyclopropane-1-carboxylic acid as a major conjugate of 1-aminocyclopropane-1-carboxylic acid, an ethylene precursor in higher plants. *Biochemical and Biophysical Research Communications* 104: 765–770.
- Houben M, Van De Poel B. 2019. 1-Aminocyclopropane-1-carboxylic acid oxidase (ACO): the enzyme that makes the plant hormone ethylene. *Frontiers in Plant Science* 10: 695.
- Karady M, Hladík P, Cermanová K, Jiroutová P, Antoniadi I, Casanova-Sáez R, Ljung K, Novák O. 2024. Profiling of 1-aminocyclopropane-1-carboxylic acid and selected phytohormones in *Arabidopsis* using liquid chromatography-tandem mass spectrometry. *Plant Methods* 20: 41.
- Kazan K. 2015. Diverse roles of jasmonates and ethylene in abiotic stress tolerance. *Trends in Plant Science* 20: 219–229.
- Koo AJ, Gao X, Daniel Jones A, Howe GA. 2009. A rapid wound signal activates the systemic synthesis of bioactive jasmonates in *Arabidopsis*. *The Plant Journal* 59: 974–986.
- Kumar D, Gautam N, Alnouti Y. 2022. Analyte recovery in LC-MS/MS bioanalysis: an old issue revisited. *Analytica Chimica Acta* 1198: 339512.
- Lancaster JE, Shaw ML. 1994. Characterization of purified γ -glutamyl transpeptidase in onions: evidence for *in vivo* role as a peptidase. *Phytochemistry* 36: 1351–1358.
- Lanneluc-Sanson D, Phan CT, Granger RL. 1986. Analysis by reverse-phase high-pressure liquid chromatography of phenylisothiocyanate-derivatized 1-aminocyclopropane-1-carboxylic acid in apple extracts. *Analytical Biochemistry* 155: 322–327.
- Li D, Mou W, Van De Poel B, Chang C. 2022. Something old, something new: Conservation of the ethylene precursor 1-amino-cyclopropane-1-carboxylic acid as a signaling molecule. *Current Opinion in Plant Biology* 65: 102116.
- Li N, Han X, Feng D, Yuan D, Huang L-J. 2019. Signaling crosstalk between salicylic acid and ethylene/jasmonate in plant defense: do we understand what they are whispering? *International Journal of Molecular Sciences* 20: 671.
- Li S, Han X, Yang L, Deng X, Wu H, Zhang M, Liu Y, Zhang S, Xu J. 2018. Mitogen-activated protein kinases and calcium-dependent protein kinases are involved in wounding-induced ethylene biosynthesis in *Arabidopsis thaliana*. *Plant, Cell & Environment* 41: 134–147.
- Li W, Li Q, Lyu M, Wang Z, Song Z, Zhong S, Gu H, Dong J, Dresselhaus T, Zhong S. 2022. Lack of ethylene does not affect reproductive success and synergid cell death in *Arabidopsis*. *Molecular Plant* 15: 354–362.
- Lizada C, Yang SF. 1979. A simple and sensitive assay for 1-aminocyclopropane-1-carboxylic acid. *Analytical Biochemistry* 100: 140–145.
- Martin MN, Cohen JD, Saftner RA. 1995. A new 1-aminocyclopropane-1-carboxylic acid-conjugating activity in tomato fruit. *Plant Physiology* 109: 917–926.
- Martin MN, Slovin JP. 2000. Purified γ -glutamyl transpeptidases from tomato exhibit high affinity for glutathione and glutathione S-conjugates. *Plant Physiology* 122: 1417–1426.
- McDonnell L, Plett JM, Andersson-Gunnerås S, Kozela C, Dugardeyn J, Van Der Straeten D, Glick BR, Sundberg B, Regan S. 2009. Ethylene levels are regulated by a plant encoded 1-aminocyclopropane-1-carboxylic acid deaminase. *Physiologia Plantarum* 136: 94–109.
- Moreau H, Zimmermann SD, Gaillard I, Paris N. 2021. pH biosensing in the plant apoplast—a focus on root cell elongation. *Plant Physiology* 187: 504–514.
- Morris DA, Lacombe NJ. 1995. Phloem transport and conjugation of foliar-applied 1-aminocyclopropane-1-carboxylic acid in cotton (*Gossypium hirsutum* L.). *Journal of Plant Physiology* 146: 429–436.
- Mou W, Kao Y-T, Michard E, Simon AA, Li D, Wudick MM, Lizzio MA, Feijó JA, Chang C. 2020. Ethylene-independent signaling by the ethylene precursor ACC in *Arabidopsis* ovular pollen tube attraction. *Nature Communications* 11: 4082.
- Müller M, Munné-Bosch S. 2011. Rapid and sensitive hormonal profiling of complex plant samples by liquid chromatography coupled to electrospray ionization tandem mass spectrometry. *Plant Methods* 7: 1–11.
- Murashige T, Skoog F. 1962. A revised medium for rapid growth and bio assays with tobacco tissue cultures. *Physiologia Plantarum* 15: 473–497.

- Nascimento FX, Rossi MJ, Glick BR. 2018. Ethylene and 1-aminocyclopropane-1-carboxylate (ACC) in plant–bacterial interactions. *Frontiers in Plant Science* 9: 338907.
- Nieuwenhuizen NJ, Chen X, Pellan M, Zhang L, Guo L, Laing WA, Schaffer RJ, Atkinson RG, Allan AC. 2021. Regulation of wound ethylene biosynthesis by NAC transcription factors in kiwifruit. *BMC Plant Biology* 21: 411.
- Pan X, Welti R, Wang X. 2010. Quantitative analysis of major plant hormones in crude plant extracts by high-performance liquid chromatography–mass spectrometry. *Nature Protocols* 5: 986–992.
- Pattyn J, Vaughan-Hirsch J, Van De Poel B. 2021. The regulation of ethylene biosynthesis: a complex multilevel control circuitry. *New Phytologist* 229: 770–782.
- Peiser G, Yang SF. 1998. Evidence for 1-(malonylamino) cyclopropane-1-carboxylic acid being the major conjugate of aminocyclopropane-1-carboxylic acid in tomato fruit. *Plant Physiology* 116: 1527–1532.
- Rao MV, Lee HI, Davis KR. 2002. Ozone-induced ethylene production is dependent on salicylic acid, and both salicylic acid and ethylene act in concert to regulate ozone-induced cell death. *The Plant Journal* 32: 447–456.
- Sanchez-Munoz R, Depaepe T, Samalova M, Hejatko J, Zaplana I, Van Der Straeten D. 2024. The molecular core of transcriptome responses to abiotic stress in plants: a machine learning-driven meta-analysis. *bioRxiv*. doi: 10.1101/2024.01.24.576978.
- Sarquis JI, Morgan PW, Jordan WR. 1992. Metabolism of 1-aminocyclopropane-1-carboxylic acid in etiolated maize seedlings grown under mechanical impedance. *Plant Physiology* 98: 1342–1348.
- Savidge RA, Mutumba GM, Heald JK, Wareing PF. 1983. Gas chromatography–mass spectroscopy identification of 1-aminocyclopropane-1-carboxylic acid in compressionwood vascular cambium of *Pinus contorta* Dougl. *Plant Physiology* 71: 434–436.
- Semenova GA. 2002. The thylakoid membrane in a wide pH range. *Journal of Plant Physiology* 159: 613–625.
- Shekhawat K, Fröhlich K, García-Ramírez GX, Trapp MA, Hirt H. 2022. Ethylene: a master regulator of plant–microbe interactions under abiotic stresses. *Cells* 12: 31.
- Shen J, Zeng Y, Zhuang X, Sun L, Yao X, Pimpl P, Jiang L. 2013. Organelle pH in the Arabidopsis endomembrane system. *Molecular Plant* 6: 1419–1437.
- Šimura J, Antoniadí I, Široká J, Tarkowská D, Strnad M, Ljung K, Novák O. 2018. Plant hormonomics: multiple phytohormone profiling by targeted metabolomics. *Plant Physiology* 177: 476–489.
- Smets R, Claes V, van Onckelen HA, Prinsen E. 2003. Extraction and quantitative analysis of 1-aminocyclopropane-1-carboxylic acid in plant tissue by gas chromatography coupled to mass spectrometry. *Journal of Chromatography A* 993: 79–87.
- Staswick PE, Tiriyaki I. 2004. The oxylipin signal jasmonic acid is activated by an enzyme that conjugates it to isoleucine in Arabidopsis. *Plant Cell* 16: 2117–2127.
- Staswick PE, Tiriyaki I, Rowe ML. 2002. Jasmonate response locus *JAR1* and several related Arabidopsis genes encode enzymes of the firefly luciferase superfamily that show activity on jasmonic, salicylic, and indole-3-acetic acids in an assay for adenylation. *Plant Cell* 14: 1405–1415.
- Suza WP, Staswick PE. 2008. The role of *JAR1* in jasmonoyl-L-isoleucine production during Arabidopsis wound response. *Planta* 227: 1221–1232.
- Tamang BG, Li S, Rajasundaram D, Lamichhane S, Fukao T. 2021. Overlapping and stress-specific transcriptomic and hormonal responses to flooding and drought in soybean. *The Plant Journal* 107: 100–117.
- Tao J-J, Chen H-W, Ma B, Zhang W-K, Chen S-Y, Zhang J-S. 2015. The role of ethylene in plants under salinity stress. *Frontiers in Plant Science* 6: 1059.
- Tsuchisaka A, Yu G, Jin H, Alonso JM, Ecker JR, Zhang X, Gao S, Theologis A. 2009. A combinatorial interplay among the 1-aminocyclopropane-1-carboxylate isoforms regulates ethylene biosynthesis in *Arabidopsis thaliana*. *Genetics* 183: 979–1003.
- US-FDA. 2018. *Bioanalytical method validation guidance for industry*. Silver Spring, MD, USA: Biopharmaceutics.
- Van De Poel B, Bulens I, Markoula A, Hertog ML, Dreesen R, Wirtz M, Vandoninck S, Oppermann Y, Keulemans J, Hell R. 2012. Targeted systems biology profiling of tomato fruit reveals coordination of the Yang cycle and a distinct regulation of ethylene biosynthesis during postclimacteric ripening. *Plant Physiology* 160: 1498–1514.
- Van Der Straeten D, Zhou Z, Prinsen E, Van Onckelen HA, Van Montagu MC. 2001. A comparative molecular-physiological study of submergence response in lowland and deepwater rice. *Plant Physiology* 125: 955–968.
- Vanderstraeten L, Depaepe T, Bertrand S, Van Der Straeten D. 2019. The ethylene precursor ACC affects early vegetative development independently of ethylene signaling. *Frontiers in Plant Science* 10: 1591.
- Vanderstraeten L, Van Der Straeten D. 2017. Accumulation and transport of 1-aminocyclopropane-1-carboxylic acid (ACC) in plants: current status, considerations for future research and agronomic applications. *Frontiers in Plant Science* 8: 38.
- Verstraete J, Strobbe S, Van Der Straeten D, Stove C. 2021. An optimized LC-MS/MS method as a pivotal tool to steer thiamine biofortification strategies in rice. *Talanta* 224: 121905.
- WADA. 2010. *Identification criteria for qualitative assays incorporating column chromatography and mass spectrometry*. Montreal, QC, Canada: World Anti-Doping Agency.
- Wang KL-C, Yoshida H, Lurin C, Ecker JR. 2004. Regulation of ethylene gas biosynthesis by the Arabidopsis ETO1 protein. *Nature* 428: 945–950.
- Xu S-L, Rahman A, Baskin TI, Kieber JJ. 2008. Two leucine-rich repeat receptor kinases mediate signaling, linking cell wall biosynthesis and ACC synthase in Arabidopsis. *Plant Cell* 20: 3065–3079.
- Yamoune A, Zdarska M, Depaepe T, Korytarova A, Skalak J, Berendzen KW, Mira-Rodado V, Tarr P, Spackova E, Badurova L. 2023. Cytokinins regulate spatially-specific ethylene production to control root growth in Arabidopsis. *bioRxiv*. doi: 10.1101/2023.01.07.522790.
- Yang SF, Hoffman NE. 1984. Ethylene biosynthesis and its regulation in higher plants. *Annual Review of Plant Physiology* 35: 155–189.
- Ziegler J, Qwegwer J, Schubert M, Erickson JL, Schattat M, Bürstenbinder K, Grubb CD, Abel S. 2014. Simultaneous analysis of apolar phytohormones and 1-aminocyclopropan-1-carboxylic acid by high performance liquid chromatography/electrospray negative ion tandem mass spectrometry via 9-fluorenylmethoxycarbonyl chloride derivatization. *Journal of Chromatography A* 1362: 102–109.

Supporting Information

Additional Supporting Information may be found online in the Supporting Information section at the end of the article.

Dataset S1 The raw data supporting this study.

Fig. S1 Calibration curves for 1-aminocyclopropane carboxylic acid (ACC), malonyl-1-aminocyclopropane carboxylic acid (MACC), glutamyl-1-aminocyclopropane carboxylic acid (GACC), and jasmonyl-1-aminocyclopropane carboxylic acid (JA-ACC).

Fig. S2 Linearity plots for 1-aminocyclopropane carboxylic acid (ACC), malonyl-1-aminocyclopropane carboxylic acid (MACC), glutamyl-1-aminocyclopropane carboxylic acid (GACC), and jasmonyl-1-aminocyclopropane carboxylic acid (JA-ACC).

Fig. S3 Phenotypes of Arabidopsis plants used for method validation.

Notes S1 Chemical synthesis strategies for malonyl-1-aminocyclopropane carboxylic acid (MACC) and glutamyl-1-aminocyclopropane carboxylic acid (GACC).

Notes S2 ^1H and ^{13}C Nuclear Magnetic Resonance (NMR) spectra for malonyl-1-aminocyclopropane carboxylic acid (MACC), glutamyl-1-aminocyclopropane carboxylic acid (GACC) and synthesis intermediate products.

Table S1 Structure, empirical formula, theoretical (calculated) and measured m/z value, including deviation from the theoretical value (ppm) of the different product ions of 1-aminocyclopropane-1-carboxylic acid (ACC), malonyl-ACC (MACC), glutamyl-ACC

(GACC), and jasmonyl-ACC (JA-ACC) obtained in the product ion scans of the protonated molecules.

Table S2 Validated selectivity for ACC and related derivatives.

Please note: Wiley is not responsible for the content or functionality of any Supporting Information supplied by the authors. Any queries (other than missing material) should be directed to the *New Phytologist* Central Office.